laxation rates are compared in a variety of matrix environments.

Registry No. Polystyrene (homopolymer), 9003-53-6.

References and Notes

(1) Klein, J. *Nature (London)* **1978**, *271*, 143.
(2) von Meerwall, E. *J. Magn. Reson.* **1982**, *50*, 409.
(3) Stejskal, E. O.; Tanner, J. E. *J. Chem. Phys.* **1965**, *42*, 288.
(4) Callaghan, P. T.; Pinder, D. N. *Macromolecules* **1983**, *16*, 968.
(5) Bernard, D. A.; Noolandi, J. *Macromolecules* **1983**, *16*, 548.
(6) Bernard, D. A.; Noolandi, J. *Macromolecules* **1982**, *15*, 1553.
(7) Callaghan, P. T.; Trotter, C. M.; Jolley, K. W. *J. Magn. Reson.* **1980**, *37*, 247.
(8) Leger, L.; Hervet, H.; Rondelez, F. *Macromolecules* **1981**, *14*, 1732.
(9) Callaghan, P. T.; Pinder, D. N. *Macromolecules* **1981**, *14*, 1334.
(10) Callaghan, P. T.; Pinder, D. N. *Macromolecules* **1984**, *17*, 431.

Diffusion Coefficients in Semidilute Solutions Evaluated from Dynamic Light Scattering and Concentration Gradient Measurements as a Function of Solvent Quality. 1. Intermediate Molecular Weights

Wyn Brown* and Robert M. Johnsen

Institute of Physical Chemistry, University of Uppsala, S-751 21 Uppsala, Sweden.

Received April 23, 1984

ABSTRACT: Photon correlation spectroscopy measurements on semidilute solutions of low (10^5) and medium (10^6) molecular weight polystyrene in good (THF, benzene), marginal (ethyl acetate), and Θ (cyclopentane) solvents are described. The autocorrelation function is treated by the cumulant method ($\bar{D}_{cum}$) and by bimodal analysis. In good solvents a main exponent (bimodal analysis) describes a molecular weight independent cooperative diffusion coefficient. A slow component, q^2 dependent, is present in small amount. In ethyl acetate two q^2-dependent modes are present. The relative amplitude of the fast mode (D_C) is strongly concentration and angle dependent. Two modes are also found in the Θ solvent, cyclopentane, again both q^2 dependent. It is concluded that for intermediate molecular weight polymers at semidilute concentrations, dynamic light scattering measurements detect contributions to the dynamic structure factor from two complementary modes: collective motions of the partly-formed pseudogel and center-of-mass translational motions. The classical gradient technique gives values equal to the cooperative diffusion coefficient in a good solvent and to an average of the two modes in a Θ solvent.

Introduction

In dynamic light scattering (QELS) on semidilute polymer solutions there is a now well-documented departure, with increasing concentration (and angle), of the intensity autocorrelation function from a single exponential. In Θ systems, however, the line shape is strongly nonexponential,[1,2,4,10] whereas the effect is less well-pronounced in good solvents.[3,6] For example, when the data are treated by the usual cumulant method, the value of the normalized second cumulant, $\mu_2/\bar{\Gamma}^2$, increases systematically as a function of both concentration and angle. As emphasized by Nose and Chu,[1] this parameter provides a measure of sample polydispersity in dilute solution. In semidilute solutions, however, trends in $\mu_2/\bar{\Gamma}^2$ instead reflect a change in the relative amplitudes of the contributing modes of relaxation. While the predictions of de Gennes' model[11] for semidilute polymer solutions have been invaluable in promoting understanding of the dynamics of transient networks, it becomes increasingly clear that this approach cannot entirely accommodate the observed complexity of the correlation function for intermediate molecular weights. The present contribution is directed toward the elucidation of the interpretation of the nonexponentiality of the spectra as a function of solvent quality and which has caused considerable speculation in the literature. It comprises extensive measurements on narrow fractions of polystyrene of low (10^5) and medium (10^6) molecular weights in good, marginal, and Θ solvents. The QELS data were generally confined to the usually probed $qR_G < 1$ region and in the concentration interval $1 < C/C^* < 10$. In all solvents the angular dependence of the correlation function was examined. The data have been analyzed by both the cumulant method[12] and bimodal analysis. These results are compared with those obtained with the classical macroscopic gradient technique.

Experimental Section

Polystyrenes. Narrow-distribution polymers were purchased from Pressure Chemical Co: PS100, $\bar{M}_w = 93\,000$, $\bar{M}_w/\bar{M}_n = 1.06$; PS300, $\bar{M}_w = 281\,000$, $\bar{M}_w/\bar{M}_n = 1.06$; PS950, $\bar{M}_w = 928\,000$, $\bar{M}_w/\bar{M}_n = 1.06$.

Solvents were spectroscopic grade (Merck, Darmstadt, FRG). The solvents were dried over freshly treated (350 °C, high vacuum) molecular sieves (3 Å, Union Carbide). Earlier measurements had revealed the presence of a slow relaxation in QELS measurements which could be eliminated by thorough drying procedures.

Solutions (QELS) were prepared by weighing. At the high concentrations used here it is not possible to remove extraneous material using centrifugation. Dust-free solutions were prepared by use of a closed-circuit filtration unit. Lower molecular weights (10^5 and 3×10^5) were filtered through 0.22-μm Fluoropore (Millipore) filters and after several hours of repeated filtration, bled off into 10-mm precision-bore NMR tubes. Dilutions were performed by filtering solvent directly into the weighed tubes. In this way a number of optically clear solutions in the range 5–20% (w/w) were prepared in each solvent. At the dilute end of the concentration range, values of the normalized second cumulant ($\mu_2/\bar{\Gamma}^2$) were ≤0.03.

However, with increasing concentration, $\mu_2/\bar{\Gamma}^2$ increased; this parameter also increased with increasing angle at a given concentration (typically in the range 0.03–0.15 as θ increased from 30° to 120°).

With higher molecular weight samples (PS950), 0.5-μm Fluoropore filters were used; otherwise the above-described procedures were employed. Solutions were in each case allowed to stand after

0024-9297/85/2218-0379$01.50/0

Table I

mol wt	solvent	$R_G \times 10^{10}$/m	C^*/% (w/w)
9.3×10^5	THF	516	0.30
	ethyl acetate	440	0.40
	cyclopentane	227	3.2
9.3×10^4	THF	130	1.64
	ethyl acetate	110	2.7
	cyclopentane	58	18.9

filtering for 1 week prior to measurement.

Dynamic Light Scattering. The experimental arrangement has been described in its essentials previously.[27]

The light source was a Coherent Radiation Model CR-4 argon ion laser containing a quartz etalon frequency stabilizer in the cavity to ensure single-mode operation at 488 nm. The detector system comprised an ITT FW 130 photomultiplier, the output of which was digitized by a Nuclear Enterprises amplifier/discriminator system. A Langley-Ford 128-channel autocorrelator was used to generate the full autocorrelation function of the scattered intensity. The correlator was interfaced to a Luxor ABC computer, programed to calculate the normalized full photon-counting time correlation function, and the data were stored on floppy disks. The data could be subsequently fitted by using three-, four-, five-, or six-parameter functions as described below. The measurements were made in the angular region corresponding to $qR_G < 1$ with the NMR tubes immersed in a large-diameter (10 cm) bath of index-matching fluid (decalin).

Values of the radius of gyration, R_G, in THF are assumed to equal those in benzene and were evaluated by using a relationship in ref 18. R_G values in cyclopentane (assumed equal to the values in cyclohexane) at Θ conditions have been estimated by using tabulated data in ref 35. R_G values in ethyl acetate are assumed to be similar to those in the marginal solvent di-*n*-butyl phthalate.[36] The scattering vector, q, is given by

$$q = (4\pi n/\lambda) \sin (\theta/2)$$

where n is the solution refractive index, λ is the wavelength of incident light, and θ is the scattering angle.

The R_G values were also used to estimate approximate C^* values according to

$$C^* = 3M/4\pi R_G{}^3 N_A$$

and these are indicated in the figures and listed in Table I. Thus for PS100 most measurements were made at $\theta = 60°$ and angular dependence was established by recording the autocorrelation function over a spectrum of angles. All experiments were performed in the homodyne mode.

It was established that the scattered signal was homodyned even for the most concentrated systems used by making experiments with and without intermixing with a reference beam. Thus a 0.1-mm-diameter glass rod was introduced into the beam in the scattering cell so that the reflected light mixed with the dynamic scattering from the solution. Under these conditions a fully heterodyned signal could be obtained, the slope being half the value found without mixing.

Classical Gradient Diffusion. Measurements were made in an apparatus designed and built at this Institute. A shearing-type cell for free diffusion, described by Claesson,[14] was employed. The schlieren optical system was used. The maximum height, h_{max}, and half-width at the inflection point ΔX were measured in a microcomparator. $(\Delta X)^2$ was plotted vs. time and the mutual diffusion coefficient determined from the slope:

$$(\Delta X)^2 = 2D_m t$$

The starting time correction was always zero within experimental error.

D was also calculated by using the height–area method. The two procedures gave D values that were identical within experimental uncertainty.

The boundary was always made between two solutions differing in concentration by ΔC = 1–2%. The diffusion coefficients then correspond to the average concentration, $\bar{C}$, across the boundary. It was established that in dilute solution the D vs. C relationship closely matched that obtained by dynamic light scattering.

Data Treatment: Bimodal Analysis

The data were fitted to the function

$$g^{(2)}(\tau) - 1 = \beta[A_1 \exp(-\Gamma_1\tau) + A_2 \exp(-\Gamma_2\tau)]^2 \quad (1)$$

after adjustment to the statistical base line, where the latter is the total number of pulses times the mean pulses per sampling time. Our model does not include an adjustable base line. From actual experiments in this and other investigations, no basis for using other than the statistical base line seems justified (which would otherwise be apparent as a trend in the residuals). In the case of a single-exponential decay with fixed base line, the decay rate is determined with greatest relative precision when the evenly spaced data cover two relaxation times. Furthermore, the addition of a third exponential term requires data of such high precision[15] that its inclusion is questionable.

For calculation purposes, eq 1 was expressed

$$Y \text{ (channel no.)} = P(1)[P(3) \exp(-P(2) \times \text{channel no.}) + (1 - P(3)) \exp(-P(4) \times \text{channel no.})]^2 \quad (2)$$

where $Y = (g^{(2)}(\tau) - 1)$, $P(1) = \beta$, an instrumental constant (interval 0–1, here $\simeq$0.65), $P(3)$ = relative amplitude of the first exponential (interval 0–1), and $P(2)$ and $P(4)$ are inverse relaxation times, expressed in channel numbers; for decay processes $1/P(2)$ and $1/P(4)$ must be positive. Since a relaxation time of less than one channel is immeasurable, $P(2)$ and $P(4)$ have an upper limit of unity.

The fitting followed an equally weighted nonlinear regression procedure according to Marquardt[16] with parameter estimates being constrained to the 0–1 interval. The program, first written in BASIC, was rewritten in FORTH for speed and compactness and the Luxor ABC microcomputer fitted with an arithmetic processor for increased speed and accuracy. In order to determine the reliability of the calculating procedure, it was used to evaluate a number of simulated experiments. When the calculating procedure was applied to real experiments (e.g., PS in THF in dilute solution) the residuals scattered randomly, and their distribution was apparently Gaussian. Figure 1a shows the residuals from a typical experiment, and Figure 1b, the same residuals after sorting in ascending order. The smooth curve in Figure 1b is the error function with the same standard deviation as the residuals. Thus normally distributed pseudo-random numbers, typical of the residuals in a real experiment, were added to a simulated experiment using parameters also typical of the real experiments. A value of 10^{-3} was used for the standard deviation of residuals (those for real experiments lie in the range $(0.5–1.5) \times 10^{-3}$).

Table II summarizes results from two sets of simulations. The first row in each set defines the ideal value of each of the four parameters. Each set comprises 24 simulated experiments, each with the same parameter values but with different errors added. The second row of the table gives the mean value of the parameter estimates for each parameter. A measure of the scatter of the estimates is found in the standard deviation, in row number three.

Each experimental analysis yields not only an estimate of the four parameters but an estimate of the "adjustability" of the parameter based on, among other things, the scatter of the residuals in that particular experiment. The "adjustability" is expressed as estimated standard deviation of that parameter. For each parameter, the average of the 24 estimates of these standard deviations is presented in the fourth row. Points to note in the table

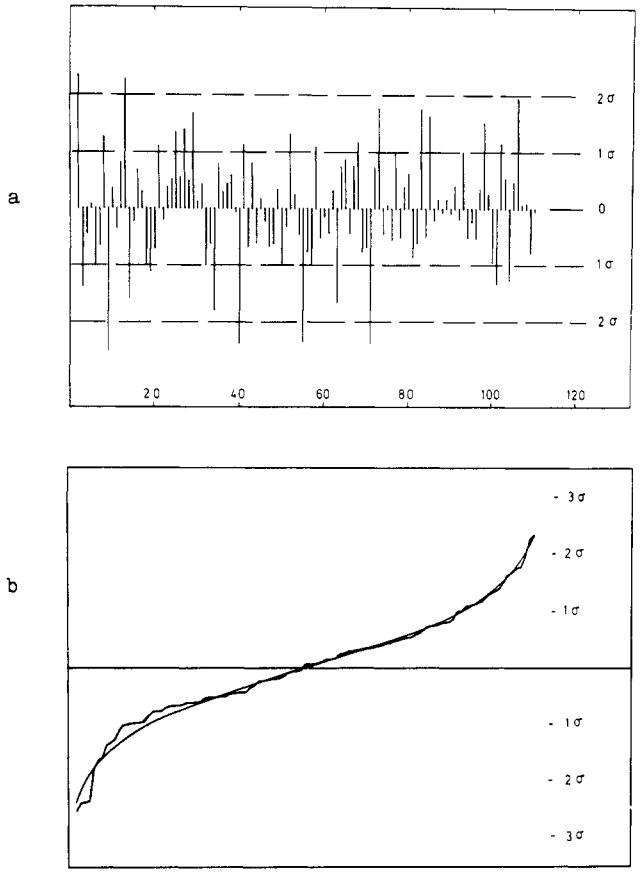

Figure 1. (a) Residuals for a typical experiment vs. channel number. The bars connect the residual and the midpoint of the diagram. The residuals are scaled in standard deviations. (b) Residuals from (a), sorted in ascending order. The error function is superimposed for comparison.

Table II[a]

	parameters			
	1	2	3	4
	Set I			
10^3 ideal value	500	11.1...	800	33.3...
10^3 av est	500	11.1	794	33
10^3 std dev est	0.54	0.21	23	1.9
10^3 av est std dev	0.62	0.25	27	2.3
	Set II			
10^3 ideal value	500	11.1...	930	33.3...
10^3 av est	500	11.1	922	33
10^3 std dev est	0.59	0.18	21	5.0
10^3 av est std dev	0.59	0.21	28	5.9

[a] Each of the three sets of simulations involves 24 "experiments". The parameters are fixed to their ideal values and normally distributed pseudorandom numbers with a standard deviation of 1×10^{-3} are added to construct 120 values. Results of the analysis are summarized as average estimate, standard deviation of the estimates, and average estimated standard deviation for each parameter.

are the following: (a) the agreement between rows 1 and 2 (the parameter estimates agree with the "true" values) and (b) the agreement between rows 3 and 4 (the "adjustability" of a parameter estimate agrees with the "variability" of the estimates).

The upper half of Table II tests a reasonable set of parameters. The system consists of 80% of a slow component, with a "relaxation time" of 90 channels. The remainder is a fast component with a relaxation time of 30 channels. The lower half tests an extreme set of parameters. Here we have only 7% of the fast component. The increased uncertainty in the determination of the rate

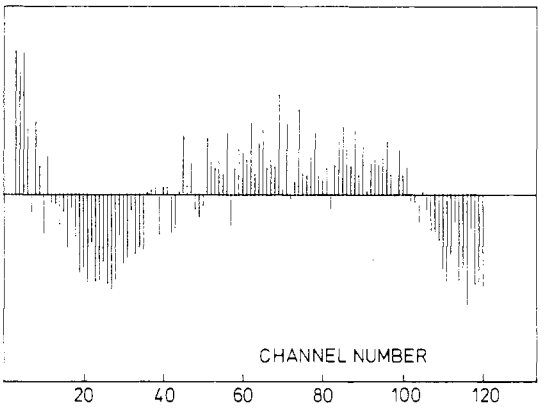

Figure 2. Residuals for a three-parameter fit (PS 950/cyclopentane; 20.8 °C; $\theta = 40°$).

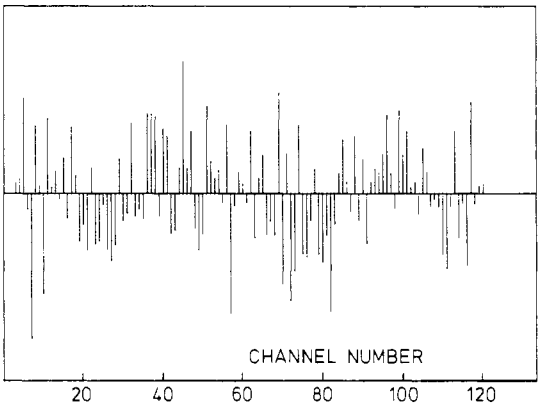

Figure 3. Residuals for a four-parameter fit of the data in Figure 2.

constant for the fast component (parameter 4) is evident. Exclusion of the data from the first few correlator channels would make the estimation of parameter 4 nearly impossible.

It is concluded that (1) parameter estimates obtained from the fitting procedure constitute "true" values without significant bias and (2) the confidence intervals for the parameter estimates are valid intervals.

A more complete discussion of the above will be published elsewhere. It may be noted that Nash and King[17] have recently described an alternative calculation procedure.

In those cases where the second rate parameter, $P(4)$, is virtually zero, the calculation procedure could be slightly altered so as to fix $P(4)$ at zero. The model to be preferred could then be judged by a function, Q, reflecting the lack of correlation between adjacent residuals. Q is defined in terms of the residuals, ϵ, for n points, as

$$Q = 1 - \frac{\sum_{i=1}^{n-1} \epsilon_i \epsilon_{i+1}/(n-1)}{\sum_{i=1}^{n} \epsilon_i \epsilon_i / n} \qquad (3)$$

If there is no apparent grouping of residuals, Q will be ≈ 1; otherwise, Q will be significantly less than one.

Such a comparison between three- and four-parameter models is illustrated in Figures 2 and 3. The inadequacy of the three-parameter model, equivalent to a single-exponential term plus floating base line, is apparent in the grouping of residuals in Figure 2. In this case, the value of Q is 0.3. Residuals from a four-parameter fit, in Figure 3, are much less prone to grouping, as reflected in a Q value of $\simeq 1$.

Results and Discussion

Two methods of data analysis (see Data Treatment) have been used to analyze the autocorrelation functions from dynamic light scattering: (a) the method of cumulants, described by Koppel,[12] which is the usual approach in QELS data interpretation, and (b) bimodal analysis, where the data were fitted to a two-exponent equation of the type of eq 1.

In dynamic light scattering on semidilute polymer solutions the well-documented departure, with increasing concentration, of the intensity autocorrelation function from an initially single exponential signals the participation of more than one mode of relaxation. As predicted by de Gennes,[11] with subsequent experimental verification,[18,19] several modes may be observable depending on the location in the qR_G vs. C/C^* plane. It is well established that there cannot be a well-defined demarcation between such modes and most measurements, due to experimental restrictions, will be made on molecular weights and with QELS parameters (angle, wavelength) that unavoidably lead to simultaneous detection of a mixture of these components. This feature has been explored in some detail by Chu and Nose[1,2] in a series of papers on the PS/*trans*-decalin Θ system.

The value of the normalized second cumulant, $\mu_2/\bar{\Gamma}^2$, is found in the present work to increase from about 0.03 at low concentrations to about 0.15 at high values—a trend that has been observed by others.[1-3,6] This systematic change in $\mu_2/\bar{\Gamma}^2$ is also apparent as a function of angle, $\mu_2/\bar{\Gamma}^2$ increasing smoothly with angle at a given concentration. As emphasized by Nose and Chu,[2] in dilute solution $\mu_2/\bar{\Gamma}^2$ provides a measure of sample polydispersity. In semidilute solutions, however, trends in this parameter instead reflect the relative change in the amplitudes of the contributing modes of relaxation.

Since the present data for low and medium molecular weights also establish two, in general, contributing modes to the dynamic structure factor over a wide range of semidilute concentrations in a number of solvent systems, it was essential to use a method such as (b) above, which makes it possible to estimate the relaxation times and their relative amplitudes. The point of agreement between techniques (a) and (b) is that $D_{cum} = \langle D \rangle$, where $\langle D \rangle$ is the weighted average of the two modes separable using (b). It is stressed here, however, that a bimodal analysis is only meaningful on runs of the highest quality, i.e., are performed on results from solutions that are rigorously dust- and particle-free. However, the limited amount of useful information contained in the autocorrelation function constrains the number of separable modes to ≤3, as a general rule, regardless of the sophistication of the analytical procedure used. Choice of bimodal (four parameter) fits in the systems described below was made by comparison with three-parameter (eq 4) fits on the basis of the Q function and on the statistical significance of the addition of a further term to eq 1 on the basis of the minimization of the reduced sum of squares of residuals, χ^2.

$$g^2(\tau) - 1 = A[\exp(-\Gamma\tau) + B]^2 \qquad (4)$$

It was found possible to make internally consistent analyses of the spectra in this way for the various systems examined (see, for example, the data for the polystyrene/THF system in Figures 4 and 5). The reliability of the analytical separation of the amplitudes/relaxation times was established by making a number of model simulations as described in the section entitled Data Treatment. It is shown that the bimodal analysis used here can consistently separate the characteristic relaxation times

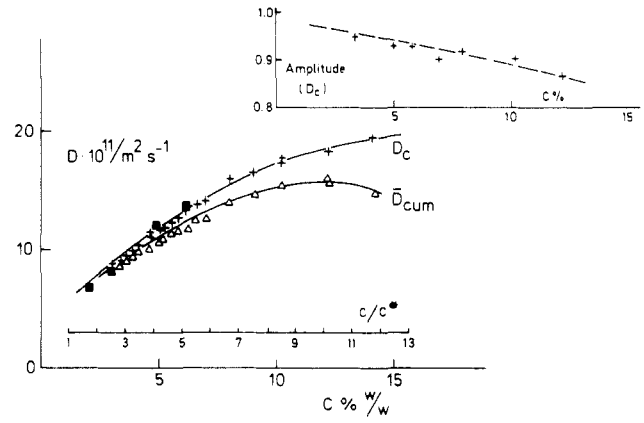

Figure 4. Data for the PS 950/THF system. D_C (+) is the main component derived from bimodal analysis. $\bar{D}_{cum}$ (Δ) is the value using the cumulant method and equals $\langle D \rangle$, the weighted average of the bimodal components. (Measurements were made at θ = 30°; qR_G = 0.48.) $\bar{D}_{CGD}$ are points (■) evaluated by classical gradient diffusion. Values of C^* are obtained by using $C^* = 3M/4\pi R_G^3 N_A$. Insert: Relative intensity contribution of the main exponent (D_C) from bimodal analysis.

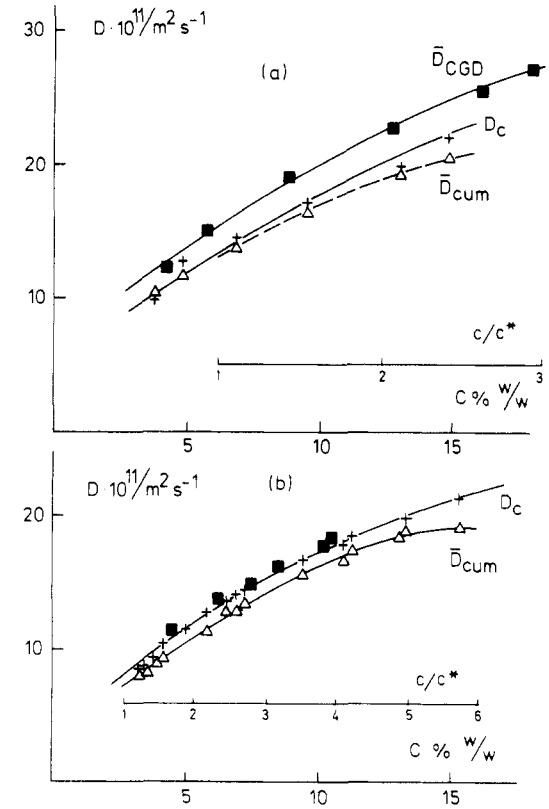

Figure 5. (a) Data for PS 100/THF (θ = 60°; qR_G = 0.24). (b) Data for PS 300/THF (θ = 60°; qR_G = 0.47). The symbols are as used in Figure 4.

when mixed in the proportions typifying the average QELS experiments described below. Thus, even when the minor component represents only 5% of the total, this mode may be consistently separated and well-defined if the relaxation times differ by at least a factor of 2. The precision decreases greatly, however, when the ratio of relaxation times falls to less than about 1.3. This latter situation arises with low molecular weights in Θ solvents.

Polydispersity may influence the present results to a minor degree, although the samples have a M_w/M_n ratio close to unity. The systematic changes, both in the normalized second cumulant and the relative amplitudes of the components, show that the autocorrelation function

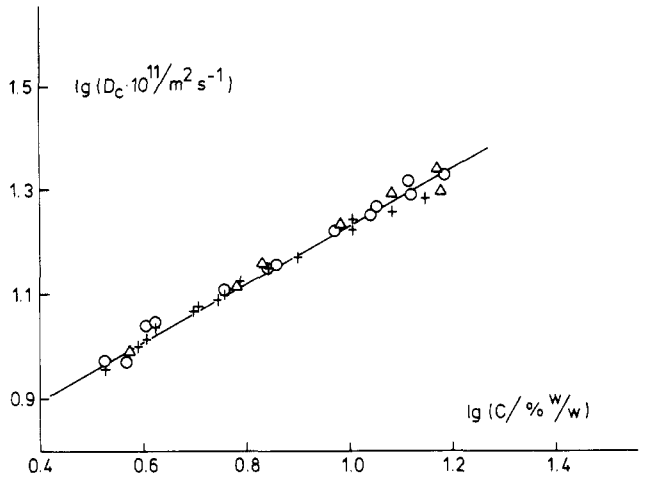

Figure 6. Double-logarithmic plot of the data for three polystyrene fractions in THF. D_C refers to the main component evaluated by bimodal analysis. ((+) 950 000; (○) 300 000; (△) 100 000). The relationship $D_C \sim C^{0.59}$ applies.

in poor solvents reflects a weighted composite of the two modes referred to above. Of course, the intensity autocorrelation function may also be nonexponential for some trivial reason such as the presence of dust or other source of local inhomogeneity. This uncertainty as to cause has resulted in some confusion in the literature[4] but should not obscure the fact that a degree of nonexponentiality is an intrinsic feature of the autocorrelation function for semidilute solutions of intermediate molecular weight polymers at usually convenient measuring conditions.

Good Solvents (THF and Benzene). The present data for three molecular weights (PS100; PS300, and PS950) in THF can be plausibly described by a three-parameter function; see eq 4. However, on the basis of the Q function (eq 3) it was deduced that bimodal analysis is more appropriate. The three-parameter fit thus gave scatter about the mean with a systematic trend and a low value of Q ($\simeq$0.5) instead of $Q \simeq 1$ as found for the bimodal fit. Comparison with addition of a base line term to eq 1 also gave no significant improvement to the fit.

The main exponent is attributed to the cooperative diffusion coefficient, D_C. The values of D_C are essentially molecular weight independent except at the highest concentrations where deviation occurs and which is more pronounced the greater is M. Thus, to a first approximation, there is a single cooperative diffusion coefficient in good solvents describing the transient gel in the semidilute region. This is consistent with the finding that the osmotic pressure is molecular weight independent[20] in good solvents.

Figure 6 illustrates the combined data in a logarithmic plot which gives the following exponent:

$$D_C \sim C^{0.59}$$

The D_C values used here are the measured quantities, D, corrected for solvent backflow according to the relationship[30]

$$D = D_C(1 - \Phi)$$

where Φ is the volume fraction of polystyrene (this correction is approximately 14% at a concentration of 15% (w/w)). The exponent is much lower than the predicted value ($\gamma = 0.75$) from scaling theory.[11] There is no tendency for the slope to increase with M as would be expected were de Gennes' value to be attained asymptotically.

It may be noted that there are extensive data suggesting that the exponent is closer to 0.6 than 0.75 (see, for example, ref 6). Data for the PS100/benzene system (Figure 7) also yield an exponent of about 0.6. This inability of the model to predict the observed variation of D_C with C serves as a possible reminder of the extent to which entanglements appear to influence the concentration dependence and which have been ignored in the simple model.

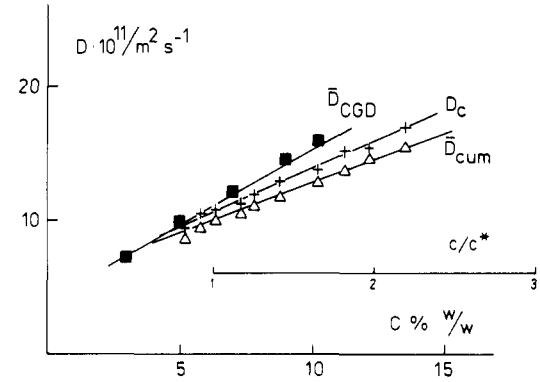

Figure 7. QELS data for PS100 in benzene analogous to those of Figures 4 and 5. Measurements at $\theta = 60°$. The relationship $D_C \sim C^{0.56}$ applies.

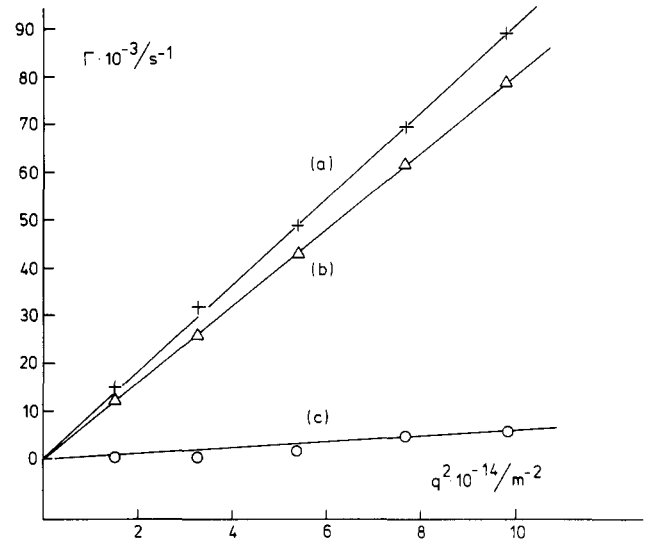

Figure 8. q^2 dependence of relaxation frequencies for PS 950/THF; $C = 4.02\%$. (a) Main component (D_C) using bimodal analysis. (b) Values from cumulant[12] analysis. (c) Minor component using bimodal analysis.

D_C approaches a plateau value as observed by Patterson et al.[21] and should thereafter decrease as frictional interactions cease to be solvent dominated and become increasingly complex due to monomer–monomer friction terms entering. Noda et al.[29] using osmotic measurements show that the crossover to the concentrated region occurs between 15 and 20% for polystyrene, irrespective of the molecular weight.

In the case of PS950, the cooperative relaxation is linearly q^2 dependent (Figure 8), substantiating its nature as a diffusional mode. Its relative amplitude decreases from about 0.97 at the lowest concentration to about 0.8 at the highest (Figure 4, insert). The slower minor component evaluated by bimodal analysis (and which is considered to be distinct from a base line term) thus has significant weighting as may also be deduced from the deviation of the cumulant values from the D_C values at higher concentrations (Figure 4). From angular measurements (Figure 8) it is concluded that there is justification for considering this component as a slow diffusional mode, although its low weight and large associated uncertainty preclude definite conclusions. As may be deduced from

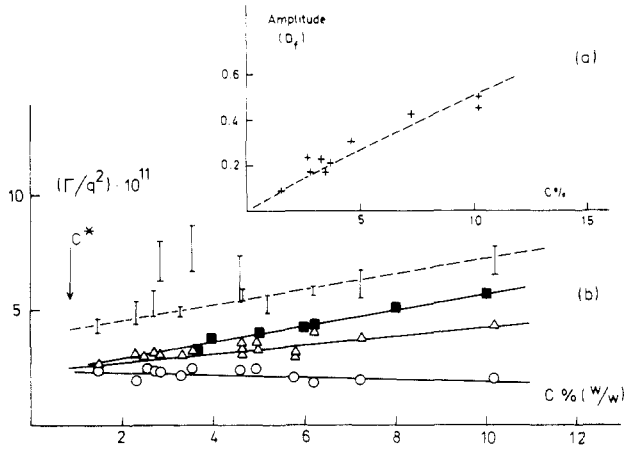

Figure 9. Data for PS950 in ethyl acetate. (Measurements at $\theta = 30°$; $qR_G = 0.64$.) (a) Relative intensity amplitude of fast mode derived by bimodal analysis as a function of concentration. (b) Fast (I) and slow (O) components obtained by bimodal analysis according to eq 1. The cumulant values (Δ) equal those formed by the weighted average ($\langle D \rangle$) of the two components. (■) Classical gradient diffusion values (D_{CGD}). The fast mode (broken line) follows the relationship $D_f \sim C^{0.28}$, derived from a log–log plot within the measurement interval.

Figure 8, this slow mode has a value of about 6×10^{-12} m^2 s^{-1} at $C = 4\%$. It has a tendency to decrease in value with increasing C. An interpretation which explains these features is that the slow mode derives from the diffusion of clusters of entangled chains.

Yu et al.[3] have also described the isolation of a linearly q^2-dependent slow relaxation of similar magnitude for semidilute solutions of linear polystyrenes in THF. They favor the viewpoint that bimodal relaxation commences above the monomer concentration at which entanglement coupling begins. This is consistent with the present data.

It appears likely that at even higher concentrations the slow component will continue to increase in amplitude and exhibit the negative concentration dependence characterizing a hydrodynamic mode described by Hwang and Cohen[7] for measurements on poly(*n*-butyl methacrylate) in MEK extending from the dilute solution to the melt. This slow mode is more readily observed at low concentrations with the more extended chains in aqueous systems.[27] We note also that Selser[6] has recently described results on poly(α-methylstyrene) in toluene which are similar to those reported here.

Recently, Amis and Han[5] used different sampling times to resolve their data on the PS/THF system into a fast (cooperative) and a slow component which was slower by several orders of magnitude. The latter could well be due to the translational motions of *groups* of chains rather than the reptation of single ones. For the present system (PS950) we were unable to isolate diffusion coefficients differing to this degree by varying the sampling time.

Results from classical gradient measurements (D_{CGD}) are given in Figure 4 and 5. For PS100 there is a pronounced deviation of the values from those derived from QELS. This trend will also be shown to apply in ethyl acetate and cyclopentane (Figure 11).

For the higher molecular weights in THF the values of D_{CGD} coincide with the values of D_C derived from QELS data, as has been earlier established by Adam and Delsanti.[18] This agreement does not, however, extend to poorer solvents (see below).

Marginal Solvent (Ethyl Acetate). Results for PS950 and PS100 in ethyl acetate are shown in Figures 9 and 11a, respectively. The major feature of Figure 9b is the presence of two distinct relaxational modes which may be obtained by bimodal analysis. The choice of the four-parameter model was based on a comparison with three- and five-parameter fits. The statistical fit using three parameters (eq 4) was much poorer than that using four-parameters (eq 1) as judged from the Q values (eq 3). A fifth parameter (base line term) was not significant. The slower mode has a slightly negative dependence on concentration and the fast, a positive and approximately linear dependence on C. A log–log plot within the measurement interval has a slope of 0.28. The feature we emphasize here, however, is the presence of two coexisting modes, where only one was anticipated. Characterization of the pseudogel slope must await improved methods for separating such components. It is not suggested, however, that complete separation has been (or can be, using the present method) achieved at the lower concentrations. Moreover, the relative intensity amplitude of the fast mode is strongly concentration dependent (Figure 9a), the autocorrelation function passing from approximately single exponential to a pronounced bimodal distribution over a short interval in concentration. It has been earlier recognized that "marginal" solvents have an apparent complexity that is not the case, to a first approximation, in good solvents, and bimodal autocorrelation functions have been described previously.[22,23] We do not find, however, that the relative intensity amplitude of the slow mode decreases with time as observed by Mathiez et al.[23] We also observe that the slow mode *decreases* in relative amplitude with increasing concentration, which contrasts with the exponential increase in the amplitude with increasing C found by these authors, suggesting the presence of local concentration inhomogeneities in their solutions. The fast mode should ultimately decrease in relative amplitude due to constraints imposed on the segmental mobility by an increased entanglement frequency as the concentrated region is approached. This has been shown by Hwang and Cohen,[7] who charted the change in the amplitude function from dilute solution up to the melt. A slow mode as noted for good solvents should then become evident.

The angular dependence of the relaxation frequency is linearly dependent on q^2 (Figure 10b), suggesting that both modes are diffusional in character. The relative intensity amplitude of the fast mode increases strongly with increasing angle (Figure 10a). It is suggested that the slow mode is the hydrodynamic quantity describing center-of-mass translational motions of the whole coil (although distinct from self-diffusion) while the fast mode corresponds to the collective segment motions of the developing pseudogel, both of which are features of autocorrelation functions obtained in experiments on samples of intermediate molecular weight.

Values of $\bar{D}_{cum}$ (=$\langle D \rangle$) in Figure 9b show an intermediate concentration dependence reflecting the relative weighting of the two modes.

Data for the low molecular weight sample (Figure 11a) were typified by single-exponential (<3% of a faster component) correlation functions up to the highest concentration (≃15%). The resulting diffusion coefficient was approximately independent of concentration. Since a single exponent was also an adequate description for this sample in the Θ solvent (see below) we conclude that a minimum chain length is conditional for observation of the pseudogel component.

For these molecular weights $\bar{D}_{cum}$ is dependent on M, which disagrees with the finding of Munch et al.[22] and Schaefer et al.[25] that there is a unique diffusion coefficient depending only on C in ethyl acetate, as is true to a first approximation in good solvents. At very high molecular

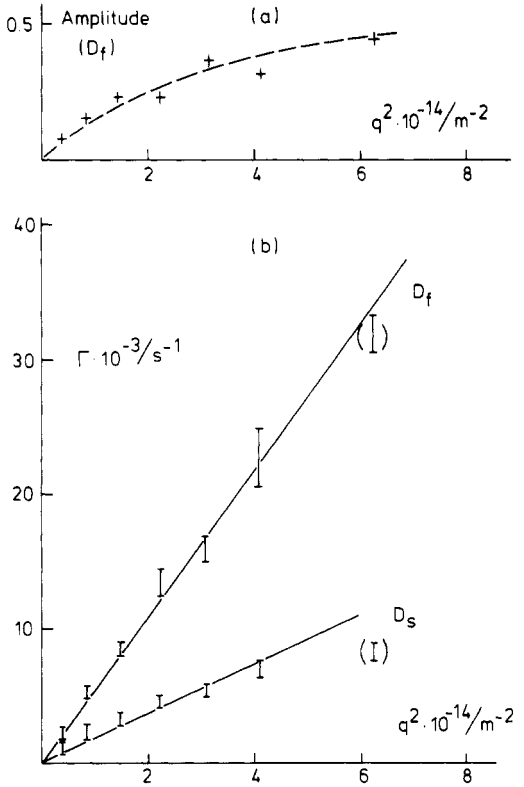

Figure 10. PS950/ethyl acetate (C = 3.29% (w/w)). q^2 dependence of (a) the amplitude of the fast mode depicted in Figure 9b and (b) fast and slow components according to Figure 9b.

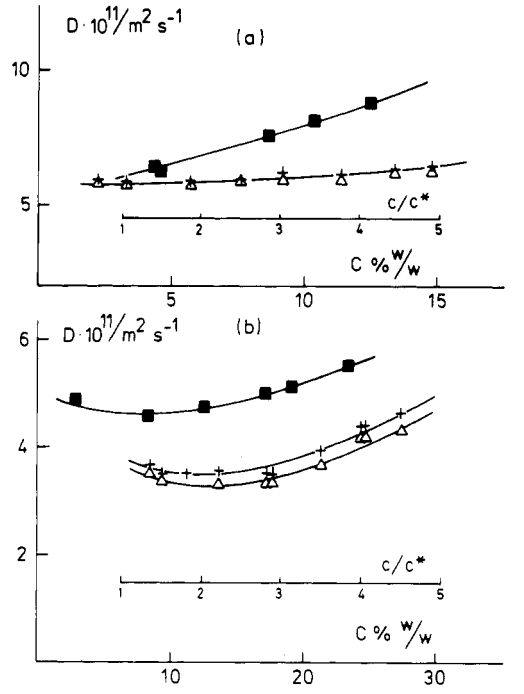

Figure 11. Data for PS100 in (a) ethyl acetate (25 °C; θ = 90°; qR_G = 0.34) and (b) cyclopentane (20.8 °C; Θ solvent; θ = 60°; qR_G = 0.24). (+) Main component (>97%) in bimodal analysis; (Δ) cumulant analysis; (■) classical gradient diffusion results. C^* = $3M/4\pi R_G{}^3 N_A$ (in ethyl acetate: $\bar{D}_{CGD} \sim C^{0.36}$).

weight, the translational mode may become too slow to constitute a meaningful component of the autocorrelation function and the latter may again be described by a single-exponential plus base line term for a given experiment.

Data from classical gradient experiments are included in Figures 9 and 11a. For PS950 in good solvents $\bar{D}_{CGD}$ falls in line with D_C (Figure 4) and in the Θ solvent (Figure 12) agrees with D_{cum}. Thus the usually assumed identity

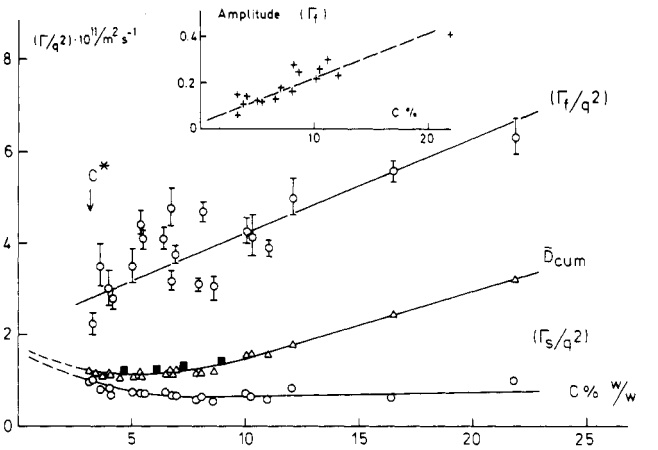

Figure 12. Data for PS950 in cyclopentane (20.8 °C; Θ conditions; measurements at θ = 40°; qR_G = 0.63). Fast (◇) and slow (○) components using bimodal analysis. $\bar{D}_{cum}$ (Δ) refers to cumulant analysis; (■) values from classical gradient diffusion ($\bar{D}_{CGD}$). The fast mode follows the relationship $D_f \sim C^{0.45}$, derived from a log–log plot within the measurement interval. The insert shows the concentration dependence of the relative intensity of the fast component.

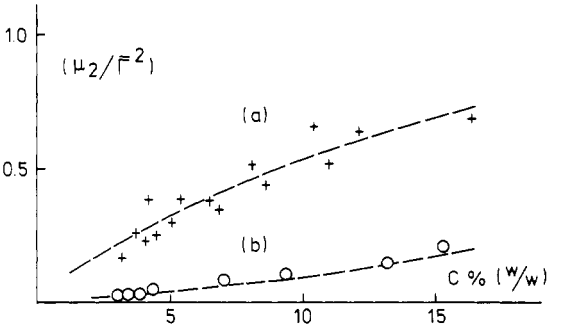

Figure 13. Dependence of the normalized second cumulant on concentration for (a) PS950/cyclopentane (20.8 °C; Θ conditions) and (b) PS950/THF (25 °C).

between $\bar{D}_{CGD}$ and D_C does not appear to hold in poorer solvents. As noted by others, $\bar{D}_{CGD}$ is molecular weight dependent and this is seen here to be a result of the important contributions to the decay of the macroscopic concentration gradient made by the different relaxational modes.

Θ Solvent (Cyclopentane, 20.8 °C). Figures 11b (PS100) and 12 (PS950) summarize the results in the Θ solvent. The spectra for PS100 are approximately single exponential over the concentration range studied, with only a small amount (<6%) of a second faster component. However, for PS950 the autocorrelation functions are strongly nonexponential and bimodal analysis readily allows resolution into two components as was the case in ethyl acetate. As for the marginal solvent, three- and five-parameter fits were both found to be less satisfactory, partly on the basis of the Q function (eq 3) and partly on the statistical lack of significance of an additional base line term. However, it must be pointed out that it is difficult to obtain precision in the definition of the modes; thus while for the individual runs the statistical fit (eq 3) was excellent, the points as a function of concentration show considerable scatter. The trend in nonexponentiality is mirrored in the concentration dependence of the normalized second cumulant shown in Figure 13a. This diagram compares this parameter with its behavior in the good solvent THF.

The fast mode (Figure 12), which is ascribed to the developing pseudogel has an approximately linear dependence on C. Within the measurement interval, a log–log

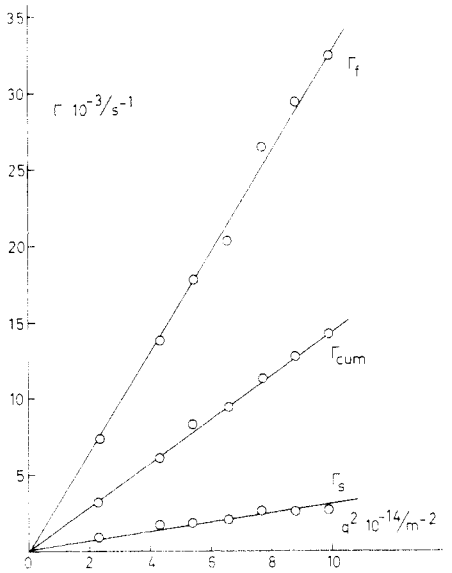

Figure 14. PS950/cyclopentane (20.8 °C) (C = 7.8% (w/w)). q^2 dependence of fast and slow modes using bimodal analysis and for cumulant evaluation.

plot has a slope of 0.46 (without subtraction of the fictive intercept (see ref 21) which would make the slope unity). Again we wish to stress the general presence of more than one mode of relaxation, rather than the value of the $D \sim C^{\gamma}$ exponent. Hecht et al.[33] have analyzed low-angle QELS data for the PS/cyclohexane system using the method of cumulants and report a value of 0.94 for the exponent. Similarly an exponent of unity could also have been derived from the present cumulant data at high C in Figure 12 but is considered to be a highly tenuous conclusion from this type of plot where it can be tempting to approximate the data to a straight line at high C and thus find an exponent of unity; see, also ref 13. Furthermore, such an exponent will only be meaningful if it can be demonstrated that *only* a single relaxational mode contributes to $S(q,t)$. The slow component is approximately independent of concentration, showing an upturn at low values toward the intercept. This dependence has the same qualitative character as that for the polymer self-diffusion coefficient,[32] which is simply related to the inverse friction coefficient. The slow component is thus ascribed to translational motions of the whole polymer coil. The slope of Γ_s/q^2 is shallower than anticipated. Possible causes will include incomplete separation of the two modes using eq 1 and also that the value of $qR_G = 0.63$ does not satisfy the condition $qR_G \ll 1$ (see ref 1). Furthermore, there may be a collapse in the hydrodynamic radius at the semidilute/concentrated crossover as discussed by Martin.[34] Supporting the contention that both fast and slow relaxations are diffusional modes, Figure 14 shows the q^2 dependence of these data. This is noteworthy since Brochard[26] has predicted a q-independent rate for the slow mode, which is regarded as a viscous relaxation owing to the long disentanglement time in comparison with a concentration fluctuation. Adam and Delsanti[10] support this view with data on very high molecular weight polystyrenes in cyclohexane. The amplitude of the fast mode increases approximately linearly with concentration (insert, Figure 12) but the rate of change is less pronounced than for the marginal solvent. Thus the translational mode is the dominant feature at all the concentrations studied. Measurements were also made in cyclopentane at temperatures of 35 and 46 °C. The increase of the relative amplitude of the fast mode is shown in Figure 15. The relaxation frequency is still strictly linearly q^2 dependent for both modes at the higher temperatures. Chu and Nose[1] report a similar variation in the amplitude of the fast mode for the PS/*trans*-decalin system. They attribute the change in the relative intensity to the change in coil dimensions with increasing solvent power, with a consequent shift in position in the $qR_G/(C/C^*)$ diagram toward the pseudogel component.

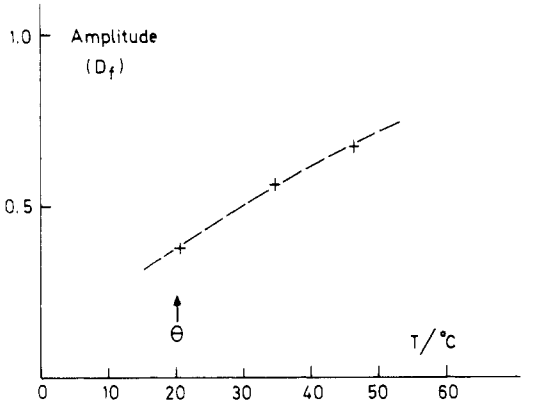

Figure 15. Relative amplitude of the fast component as a function of temperature (PS950/cyclopentane; θ = 40°).

The coefficient evaluated by the cumulant method initially decreases followed by a monotonic increase as usually observed[4] over extended ranges in concentration. The shallow minimum is thus viewed as deriving from the increased weighting of the segment motions compared to the center-of-mass motions above C^*. The classical gradient results fall into line with the values of $\bar{D}_{cum}$ (=$\langle D \rangle$). It is noted that the values of $\bar{D}_{CGD}$ are significantly molecular weight dependent (cf. Figures 11b and 12), which derives from contributions from the translational mode since both segmental and translational motions will contribute to the relaxation of the concentration gradient. This casts doubt on the validity of using D_{CGD} to test, for example, scaling law predictions.[13] The present results are similar to those reported by Chu and Nose,[1] who examined the polystyrene/*trans*-decalin system. We wish, however, to emphasize the important role of the molecular weight. Single-exponential correlation functions are found for low M (10^5) and this is also assumed[10] although not unambiguously demonstrated for extremely high molecular weights. Thus it is seen that it is only for intermediate values of M that the partly developed pseudogel is observable over a wide range of concentration; the transient network is still sufficiently labile to permit substantial translational mobility. As the concentrated region is approached we may anticipate the appearance of a very slow relaxation similar to that noted for good solvents.

Amis et al.[31] have, after submission of this paper, described measurements on the PS/cyclohexane system and describe detection of fast and slow components using widely differing sampling times. However, as was also the case in the PS/THF system, we have been unable to isolate diffusion coefficients differing by several orders of magnitude by varying the sample time in our Θ system using a similar molecular weight and concentration to Amis et al.

Conclusions

The main point presented is that, for a given system, there will be a window of molecular weight where dynamic light scattering measurements detect contributions to the dynamic structure factor from two complementary modes in semidilute solutions. The transition from a good via marginal to a Θ solvent then involves a progressive change in the weighting of the two components which reflect on the one hand collective motions of the developing pseu-

dogel and on the other center-of-mass translational motions of the coil itself. In good solvents the former dominates almost exclusively while the translational mode dominates in a Θ solvent. In the good solvent, however, a very slow relaxation also becomes evident and complicates the picture at the highest concentration, bordering the concentrated region. There is still controversy as to its origin but feasibly it is related to the motions of clusters of entangled chains.

With low M ($M = 10^5$) the autocorrelation function is single exponential independent of solvent quality. Also, at very high M ($M \sim 10^7$) the translational motions may become too slow to be observed in the usual QELS experiment. The results of Adam and Delsanti[10,18] have been interpreted as a single diffusive mode on samples of $M \simeq 2.4 \times 10^7$ in both good and poor solvents although in their Θ system a slow, q-independent relaxation is monitored with long sampling times. Nevertheless, recent QELS results[37] on very high molecular weight polystyrenes in both good and Θ solvents show that two modes are present throughout the experimentally accessible region of $qR_G/(C/C^*)$ space.

Under Θ conditions at concentrations far above C^*, both modes are detectable with intermediate molecular weights. Thus a too rigid view of C^* as a concentration above which one only observes the transient gel at $qR_G < 1$ is unwarranted.

Marginal solvents show features akin to Θ solvents in that the autocorrelation functions are typically bimodal. The data suggest a limited value in the concept of the "marginal" solvent, the differences being of degree rather than kind. The substantial contribution from a hydrodynamic mode in poorer solvents explains why both $\bar{D}_{CGD}$ and $\bar{D}_{cum}$ are molecular weight dependent in such media. Also the nonidentity of D_C and $\bar{D}_{cum}$ at intermediate molecular weights makes the latter as well as time-averaged quantity $\bar{D}_{CGD}$ less suitable for testing theoretical models for the semidilute region which assume a specific mode. Since most measurements are made for experimental reasons using such samples, this is a major reservation.

The data presented here make it possible to reconcile the apparently divergent views that have appeared in the literature concerning fast and slow modes on the one hand and the refined demands of the limiting pseudogel model on the other. Intermediate molecular weights present a complex problem where one has to consider the interplay between the hydrodynamic motions of entangled chains and the segmental dynamics of the partly formed pseudogel. Recently a step has been taken by Ronca[28] in this direction, using a model which specifically includes the features of entanglements and their influence on the autocorrelation function.

Acknowledgment. We are grateful to G. Svensk for his skilful assistance in performing the gradient diffusion measurements. This work was supported by a grant from the Swedish Forest Products Research Laboratory, Stockholm.

References and Notes

(1) Chu, B.; Nose, I. *Macromolecules* **1980**, *13*, 122.
(2) Nose, I.; Chu, B. *Macromolecules* **1979**, *12*, 590, 599.
(3) Yu, T. L.; Reihanian, H.; Jamieson, A. M. *Macromolecules* **1980**, *13*, 1590.
(4) Munch, J.-P.; Hild, G.; Candau, S. J. *Macromolecules* **1983**, *16*, 71.
(5) Amis, E.; Han, C. C. *Polymer* **1982**, *23*, 1042.
(6) Selser, J. C. *J. Chem. Phys.* **1983**, *79* (2), 1044.
(7) Hwang, D.-h.; Cohen, C. *Macromolecules* **1984**, *17*, 1679.
(8) Nishio, I.; Wada, A. *Polym. J.* **1980**, *12*, 145.
(9) Brown, W.; Johnsen, R. M.; Stilbs, P. *Polym. Bull.* **1983**, *9*, 305.
(10) Adam, M.; Delsanti, M. *J. Phys. (Paris), Lett.* **1984**, *45*, L-279.
(11) de Gennes, P.-G. *Macromolecules* **1976**, *9*, 587, 594.
(12) Koppel, D. E. *J. Chem. Phys.* **1972**, *57*, 4814.
(13) Roots, J.; Nyström, B. *Macromolecules* **1980**, *13*, 1595.
(14) Claesson, S. *Nature (London)* **1946**, *158*, 834.
(15) Lanczos, C. "Applied Analysis"; Prentice-Hall: Englewood Cliffs, NJ, 1956.
(16) Marquardt, D. W. *SIAM J. Appl. Math.* **1963**, *11*, 431.
(17) Nash, P. J.; King, T. A. *J. Chem. Soc., Faraday Trans. 2* **1983**, *79*, 989.
(18) Adam, M.; Delsanti, M. *Macromolecules* **1977**, *10*, 1229.
(19) Munch, J.-P.; Lemarchal, R.; Candau, S. J.; Herz, J. *J. Phys. (Paris)* **1977**, *38*, 1499.
(20) Noda, I.; Kato, N.; Kitano, T.; Nagasawa, M. *Macromolecules* **1981**, *14*, 668.
(21) Patterson, G. D.; Jarry, J. P.; Lindsey, C. P. *Macromolecules* **1980**, *13*, 668.
(22) Munch, J. P.; Candau, S.; Herz, J.; Hild, G. *J. Phys. (Paris)* **1977**, *38*, 971.
(23) Mathiez, P.; Mouttet, C.; Weisbuch, G. *J. Phys. (Paris)* **1980**, *41*, 519.
(24) Carlfors, J.; Rymdén, R.; Nyström, B. *Polymer* **1983**, *24*, 263.
(25) Schaefer, D. W.; Joanny, J. F.; Pincus, P. *Macromolecules* **1980**, *13*, 1280.
(26) Brochard, F. *J. Phys. (Paris)* **1983**, *44*, 39.
(27) Brown, W. *Macromolecules* **1984**, *17*, 66.
(28) Ronca, G. *J. Chem. Phys.* **1983**, *79*, 1031.
(29) Noda, I.; Higo, Y.; Ueno, N.; Fujimoto, T. *Macromolecules* **1984**, *17*, 1055.
(30) Geissler, E.; Hecht, A. M. *J. Phys. Lett.* **1979**, *40*, L-173.
(31) Amis, E. J.; Han, C. C.; Matsushita, Y. *Polymer* **1984**, *25*, 650.
(32) Brown, W.; Stilbs, P.; Johnsen, R. M. *J. Polym. Sci., Polym. Phys. Ed.* **1983**, *21*, 1029.
(33) Hecht, A. M.; Bohidar, H. B.; Geissler, E. *J. Phys. (Paris), Lett.* **1984**, *45*, L-121.
(34) Martin, J. E. *Macromolecules* **1984**, *17*, 1279.
(35) Adam, M.; Delsanti, M. *J. Phys. (Paris)* **1980**, *41*, 721.
(36) Candau, S. J.; Butler, I.; King, T. A. *Macromolecules*, in press.
(37) Brown, W. *Macromolecules*, in press.